



OPEN ACCESS

EDITED BY

Aurore Claude-Taupin,
INSERM U1151 Institut Necker Enfants Malades,
France

REVIEWED BY

Thomas Anthony Ryan,
Synganture Discovery Ltd., United Kingdom
Shirisha Nagotu,
Indian Institute of Technology Guwahati, India

*CORRESPONDENCE

Patricia Boya,
✉ patricia.boya@unifr.ch

RECEIVED 05 July 2024

ACCEPTED 02 September 2024

PUBLISHED 11 September 2024

CITATION

Jiménez-Loygorri JI, Jiménez-García C,
Viedma-Poyatos Á and Boya P (2024) Fast and
quantitative mitophagy assessment by flow
cytometry using the *mito*-QC reporter.
Front. Cell Dev. Biol. 12:1460061.
doi: 10.3389/fcell.2024.1460061

COPYRIGHT

© 2024 Jiménez-Loygorri, Jiménez-García,
Viedma-Poyatos and Boya. This is an open-
access article distributed under the terms of the
[Creative Commons Attribution License \(CC BY\)](https://creativecommons.org/licenses/by/4.0/).
The use, distribution or reproduction in other
forums is permitted, provided the original
author(s) and the copyright owner(s) are
credited and that the original publication in this
journal is cited, in accordance with accepted
academic practice. No use, distribution or
reproduction is permitted which does not
comply with these terms.

Fast and quantitative mitophagy assessment by flow cytometry using the *mito*-QC reporter

Juan Ignacio Jiménez-Loygorri¹, Carlos Jiménez-García²,
Álvaro Viedma-Poyatos¹ and Patricia Boya^{1,2*}

¹Department of Cellular and Molecular Biology, Centro de Investigaciones Biológicas Margarita Salas, CSIC, Madrid, Spain, ²Department of Neuroscience and Movement Science, Faculty of Science and Medicine, University of Fribourg, Fribourg, Switzerland

Mitochondrial quality control is finely tuned by mitophagy, the selective degradation of mitochondria through autophagy, and mitochondrial biogenesis. Removal of damaged mitochondria is essential to preserve cellular bioenergetics and prevent detrimental events such as sustained mitoROS production, pro-apoptotic cytochrome c release or mtDNA leakage. The array of tools available to study mitophagy is very limited but in constant development. Almost a decade ago, we developed a method to assess mitophagy flux using MitoTracker Deep Red in combination with lysosomal inhibitors. Now, using the novel tandem-fluorescence reporter *mito*-QC (mCherry-GFP-FIS1¹⁰¹⁻¹⁵²) that allows to differentiate between healthy mitochondria (mCherry⁺GFP⁺) and mitolysosomes (mCherry⁺GFP⁻), we have developed a robust and quantitative method to assess mitophagy by flow cytometry. This approach has been validated in ARPE-19 cells using PINK1/Parkin-dependent (CCCP) and PINK1/Parkin-independent (DFP) positive controls and complementary techniques. Furthermore, we show that the *mito*-QC reporter can be multiplexed, especially if using spectral flow cytometry, to simultaneously study other cellular parameters such as viability or ROS production. Using this technique, we evaluated and characterized two prospective mitophagy inducers and further dissected their mechanism of action. Finally, using *mito*-QC reporter mice, we developed a protocol to measure mitophagy levels in the retina *ex vivo*. This novel methodology will propel mitophagy research forward and accelerate the discovery of novel mitophagy modulators.

KEYWORDS

FACS, mitochondria, autophagy, retina, SI, Fisetin, phenanthroline

Introduction

Mitophagy is a subtype of selective autophagy that leads to the degradation and recycling of whole mitochondria. It can be further subdivided in two main pathways: PINK1/Parkin-dependent or receptor-mediated mitophagy. PINK1/Parkin-dependent mitophagy is traditionally triggered by loss of mitochondrial membrane potential

Abbreviations: $\Delta\Psi_m$, Mitochondrial membrane potential; AMD, Age-related macular degeneration; BNIP3, BCL2/adenovirus E1B 19 kDa protein-interacting protein 3; BNIP3L/NIX, BCL2/adenovirus E1B 19 kDa protein-interacting protein 3-like; CCCP, Carbonyl cyanide m-chlorophenyl hydrazine; DFP, Deferiprone; FIS1, Mitochondrial fission 1 protein; GFP, Green fluorescent protein; HIF-1 α , Hypoxia-inducible factor 1- α ; MFI, Mean fluorescence intensity; PINK1, PTEN-induced kinase 1; OMM, Outer mitochondrial membrane; ROS, Reactive oxygen species; RPE, Retinal pigment epithelium; SI, Sodium iodate.

($\Delta\Psi_m$) (Narendra et al., 2010). The PINK1 kinase is recruited to the outer mitochondrial membrane (OMM) where, in homeostatic conditions, is translocated through the intermembrane space, processed by the peptidase MPP and sent back to the cytosol for degradation via proteasome (Hasson et al., 2013). Mitochondrial depolarization (loss of $\Delta\Psi_m$) uncouples PINK1 translocation, and it accumulates in the OMM. PINK1 then phosphorylates basally-ubiquitinated OMM proteins at Ubiquitin^{Ser65} and the analogous residue of Parkin, an E3 ligase that will further poly-ubiquitinate OMM proteins (Narendra et al., 2008). These events lead to a positive feedback loop that amplifies the targeting signals for mitophagy. Adaptor proteins with a ubiquitin-binding domain, such as CALCOCO2/NDP52, OPTN or SQSTM1/p62 (Lazarou et al., 2015), will recognize ubiquitinated proteins and recruit autophagy initiation machinery (Nguyen et al., 2016).

Receptor-mediated mitophagy is ubiquitin-independent and can also be triggered by hypoxia or developmental cues (Esteban-Martinez et al., 2017a). It is mediated by adaptor proteins that contain both a mitochondria-targeting sequence (MTS) and a LC3-interacting domain (LIR), namely BNIP3, BNIP3L/NIX, FUNDC1 or FKBP8 (Teresak et al., 2022). In recent years, it has been identified that other mechanisms such as cardiolipin externalization or changes in OMM lipid composition can also lead to direct recognition by LC3 (Teresak et al., 2022). Nonetheless, all pathways lead to mitochondria being engulfed into an autophagosome, which will later fuse with a lysosome to ensure degradation of its cargo.

Our lab has previously described a method to assess mitophagic degradation by flow cytometry using MitoTracker DeepRed (Mauro-Lizcano et al., 2015; Esteban-Martinez et al., 2017b). Even though it has been widely used and enables analysis of mitophagy flux, it still has some limitations. For example, a simultaneous induction of mitochondrial biogenesis might mask small but robust increases on mitophagy and use of lysosomal inhibitors is required (Esteban-Martinez et al., 2017b). The development of tandem fluorescent reporters has changed the way we analyze autophagy, as it allows us to monitor effective degradation inside acidic lysosomes using a combination of pH-sensitive (GFP, Keima) and pH-insensitive (mCherry) fluorescent proteins fused to a targeting sequence. Different mitophagy reporters such as MitoTimer, mtKeima or *mito*-QC have been developed, the latter also allowing fixation for downstream immunocytochemistry analysis (Jiménez-Loygorri et al., 2023; Jimenez-Loygorri and Boya, 2024).

The *mito*-QC reporter consists of a fusion protein containing mCherry-GFP-FIS1^{101–152}, that targets the OMM. In steady-state conditions, both mCherry and GFP fluoresce in the membrane of healthy mitochondria (Figure 1A) (McWilliams et al., 2018). Upon delivery of mitochondria to the lysosomes for degradation, acidic pH quenches GFP and mitolysosomes can be identified as mCherry-only puncta (Figure 1A). We have previously described the use of *mito*-QC to assess mitophagy levels by confocal immunofluorescence (Rosignol et al., 2020; Figueiredo-Pereira et al., 2023; Jimenez-Loygorri and Boya, 2024), however this procedure is time- and resource-consuming. In the present manuscript, we describe a medium-throughput protocol to assess simultaneously mitophagy and mitochondrial mass by flow

cytometry *in vitro* and in *ex vivo* retinal cultures and highlight the possibility of performing more complex assays and targeted screens by multiplexing with additional fluorescent probes.

Materials and methods

Herein, we present an optimized traditional and spectral flow cytometry protocol that provides sensitive simultaneous readouts of mitophagy and mitochondrial mass using tandem fluorescent reporters like *mito*-QC. This assay can be performed *in vitro* or using organotypic *ex vivo* culture and may be multiplexed to analyze other parameters such as reactive oxygen species (ROS) production or viability.

Cell lines

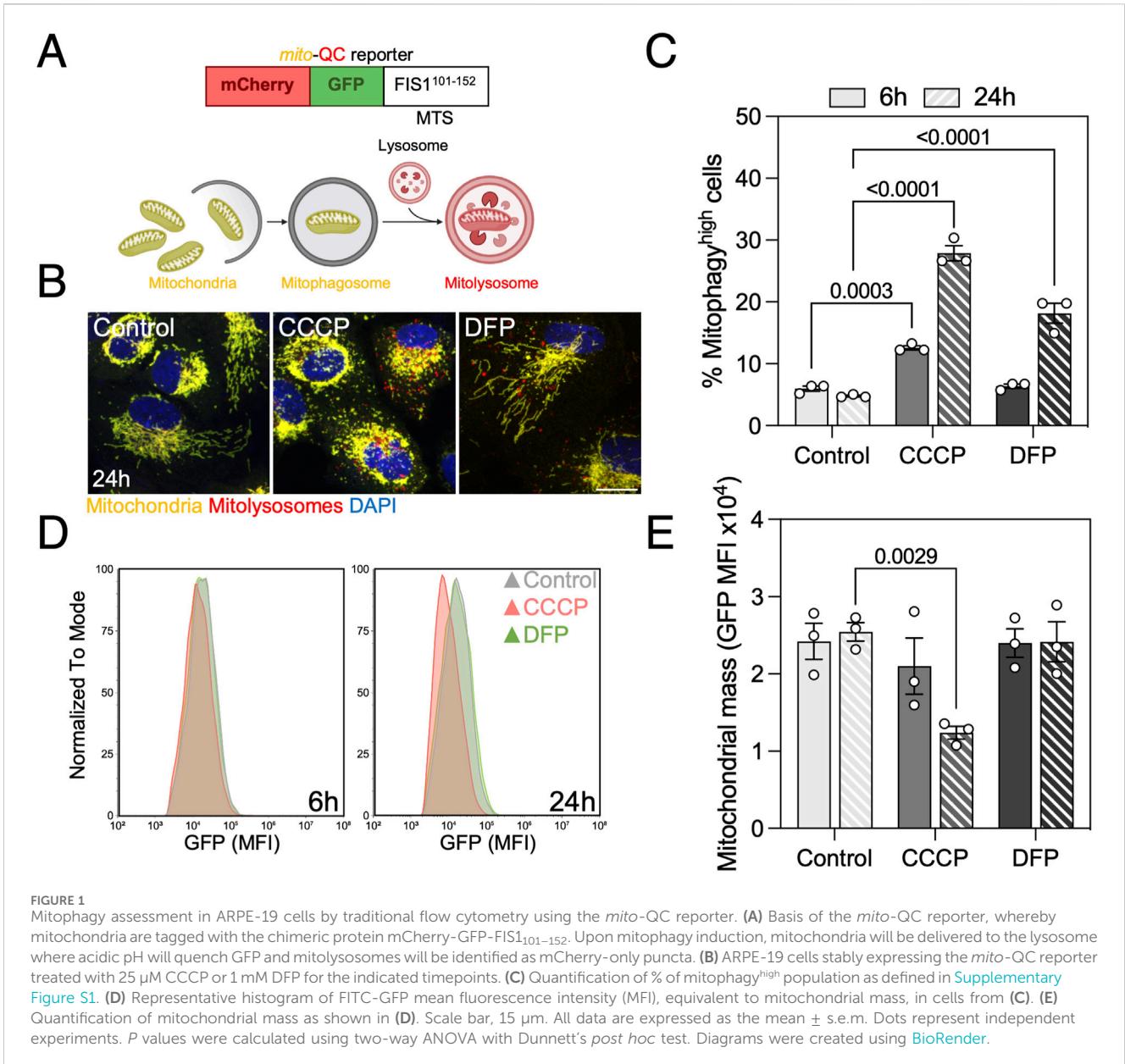
ARPE-19 cells (Dunn et al., 1996) stably expressing the *mito*-QC reporter were generated by retroviral transfection in the laboratory of Dr. Ian G. Ganley as previously described (Montava-Garriga et al., 2020) and maintained in DMEM: F-12 medium (Gibco, 41966029, 21765037) supplemented with 15% FBS (Merck, F7524), 2 mM L-glutamine (Gibco, 25030081), and 1 U/mL Pen/Strep antibiotics (Gibco, 15140122) in a humidified incubator at 37°C, 5% CO₂. To ensure stable expression of the reporter, selection was performed by adding 800 ug/mL Hygromycin B (Gibco, 10453982) after every passage.

Seeding and treatments

For flow cytometry or immunofluorescence experiments, 5–6 × 10⁴ cells per well were seeded in a 24-well plate the day before the experiment and left to adhere overnight. For western blot analysis, 3 × 10⁵ cells were seeded in a 6-well plate and left to adhere overnight. Treatments were added for the indicated timepoints at the following concentrations: 25 μM CCCP (Carbonyl cyanide m-chlorophenyl hydrazone; 25 mM stock in DMSO; Merck, C2759), 1 mM DFP (Deferiprone; 125 mM stock in sterile H₂O; Merck, 379409), 10 μM Fisetin (10 mM stock in EtOH; Merck, F4043), 50 μM Phenanthroline (50 mM stock in DMSO; Merck, 131377), 20 mM SI (Sodium iodate; 333 mM fresh stock in DMEM; Merck, S4007), 750 μM H₂O₂ (30% stock in DMEM; Fluka, 95300).

Cell sample preparation

1. Medium containing floating dead cells was collected in a standard plastic flow cytometry tube.
2. Cells were washed with 500 μL of sterile PBS 1X to remove FBS residue and PBS was also collected.
3. 150 μL of 0.05% Trypsin (Gibco, 11500636) was added per well and cells were incubated for 5' in an incubator at 37°C and 5% CO₂. Verify that cells have detached from the bottom of the well using a brightfield microscope.
4. 500 μL of FBS-containing complete medium were added to each well to inactivate Trypsin.



5. Cells were collected in the flow cytometry tube and pelleted by centrifugation at 1,000 g for 5'.
6. Supernatant was discarded and 100–200 μ L of complete medium was added to each tube. For selected experiments, cells were incubated with 1 nM MitoTracker Deep Red (Invitrogen, M22426), 1 μ M MitoSOX Red (Invitrogen, M36008), for 30' min or 1:2,000 ViaDye Red (Cytex, R7-60008), CellROX Deep Red 5 μ M (Invitrogen, C10433) for 15' at 37°C and 5% CO₂.
7. Samples were resuspended by gentle shaking and, if necessary, 50 μ L of 5X DAPI (4',6-diamidino-2-phenylindole; Merck, D9542) were added to each tube, reaching a final concentration of 1 μ g/mL, for viable population selection. If required, e.g. working with UV-autofluorescent compounds, there are far red-emitting nuclear dyes available such as TO-PRO-3 (Thermo Fisher, T3605).
8. Tubes were kept in ice until flow cytometry analysis.

Retina dissection and ex vivo culture

C57BL/6J mice expressing the *mito-QC* reporter ubiquitously were generated and provided by Dr. Ian G. Ganley ([McWilliams et al., 2018](#)). Organotypic *ex vivo* retina culture was performed as previously described ([Gomez-Sintes et al., 2017](#)). Briefly, mice were sacrificed by cervical dislocation and both eyes were enucleated using curved forceps. Using Vannas scissors, a circular incision was made along the limbus and both cornea and lens were removed using fine forceps. The optic nerve was sectioned and the neuroretina was isolated by gently pulling from the RPE/choroid-containing eyecup. Retinas were cultured in flotation in a 24-well plate and maintained in DMEM supplemented with 1 μ M Insulin (Merck, I2643), 2 mM L-Glutamine, 100 U/mL penicillin and 0.1 mg/mL streptomycin. Treatments were added for the indicated timepoints at the following concentrations: 25 μ M

CCCP (25 mM stock in DMSO), 1 mM DFP (125 mM stock in sterile H₂O).

Ex vivo retina sample preparation

1. Similarly, medium containing floating dead cells was collected in a standard plastic flow cytometry tube.
2. Whole retinas were washed with 500 μ L of sterile PBS 1X to remove medium residue and PBS was also collected.
3. 300 μ L of 5 mg/mL Trypsin in HBSS (Gibco, 14170-088) was added per well and retinas were incubated for 5–10' in an incubator at 37°C and 5% CO₂.
4. 900 μ L of 10% FBS in HBSS were added to each well to inactivate Trypsin and retinas were dissociated by gentle pipetting using a p1000 tip (10–20 times).
5. Single cell suspension was collected in the flow cytometry tube and pelleted by centrifugation at 1,000 g for 5'.
6. Supernatant was discarded and 200 μ L of complete medium was added to each tube.
7. Samples were resuspended by gentle shaking and 50 μ L of 5X DAPI was added to each tube, reaching a final concentration of 1 μ g/mL, for viable population selection.
8. Tubes were kept in ice until flow cytometry analysis.

Conventional flow cytometer setup and gating

Using a CytoFLEX S V4-B2-Y4-R3 Flow Cytometer (Beckman Coulter), at least 10,000 events were acquired using mCherry-PI (610/20), FITC-GFP (525/40), PB450-DAPI (450/45) and APC (660/10) emission filters. Gating of the viable cell population was performed as shown in [Supplementary Figures S1, S3](#). Control cells were used to set the threshold of mitophagy^{high} population defined by a mCherry/GFP ratio of ~5%. The percentage of DAPI⁻ cells, mitophagy^{high} cells, FITC-GFP MFI and APC MFI were exported for downstream analysis performed using CytExpert v1.2 (Beckman Coulter).

Spectral flow cytometer setup and gating

Using a Cytek Aurora equipped with five lasers (Cytek Biosciences), at least 10,000 events were acquired. Similarly, control cells were used to set the threshold of mitophagy^{high} population defined by a mCherry/GFP ratio of ~5%. Wild-type, control cells and unstained cells were used to set the gates and spectra for every probe ([Supplementary Figure S5](#)). Analysis was performed using SpectroFlo (Cytek Biosciences) for raw data unmixing and downstream analysis was performed using Flowjo v10.10 (BD Biosciences).

Immunofluorescence

ARPE-19 were seeded on glass coverslips, treated as indicated and fixed using 3.7% PFA containing 175 mM HEPES (Gibco,

15630) at pH 7.0 for 15 min. Cells were incubated with 1 μ g/mL DAPI in PBS pH 7.0 for 15 min, washed 3 times with PBS pH 7.0 and mounted using or ProLong Diamond (Thermo Fisher, P36961). Images were captured with a 0.5- μ m z-step using a Leica TCS SP8 confocal microscope equipped with a \times 63 immersion objective.

Protein isolation, quantification and western blot

Adherent cells were scraped in cold RIPA lysis buffer (Merck, R0278) supplemented with protease and phosphatase inhibitors. Protein concentration was determined using the Pierce BCA Protein Assay (Thermo Fisher, 23225) following the manufacturer's instructions. Total protein extract (15–30 μ g) was supplemented with 4X Laemmli loading buffer (Bio-Rad, 1610747) and resolved using Any kD Criterion TGX Precast Stain-free gels (Bio-Rad, 5678124). Proteins were transferred to 0.2 μ m PVDF membranes using a TransBlot Turbo Transfer System (Bio-Rad) and total protein was quantified using Ponceau S staining (Merck, 78376). Membranes were blocked with 5% non-fat milk in TBS-T (0.5% Tween-20 (Bio-Rad, 1706531) in PBS) for 1 h. Membranes were then incubated overnight at 4°C in primary antibodies diluted 1:1,000 ([Supplementary Table S1](#)) in 5% BSA in TBS, and subsequently for 1 h at room temperature in secondary antibodies diluted 1:2,000 in TBS-T ([Supplementary Table S1](#)). Membranes were developed using Pierce ECL Western Blotting substrate (Thermo Fisher, 32106) or Amersham ECL Prime (Cytiva, 10308449) and x-ray film (AGFA) using a CURIX 60 Processor (AGFA).

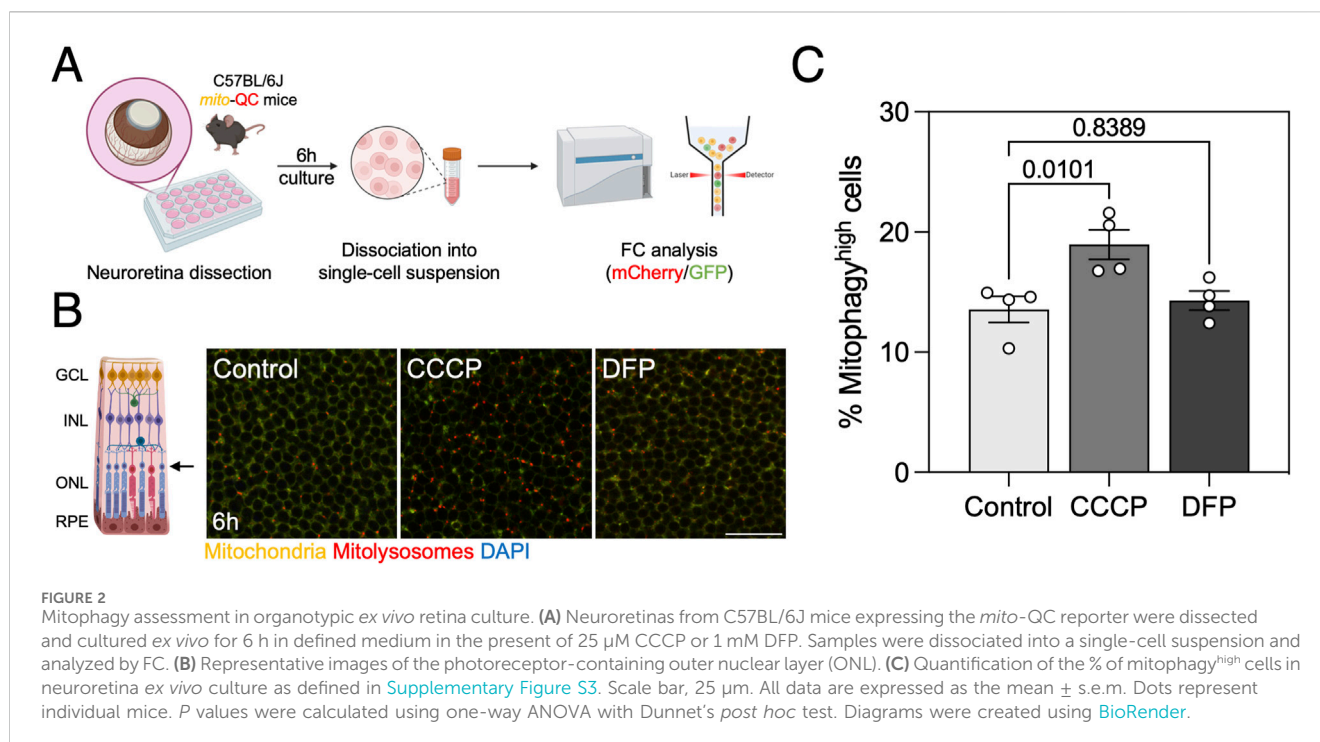
Statistical analysis

Data shown in figures represents the mean \pm s.e.m. of at least three independent experiments with biological replicates. Differences between groups were assessed using Student's *t*-test (two groups), one-way or two-way ANOVA (more than two groups) with appropriate *post hoc* tests. A *P*-value under 0.05 was considered statistically significant and exact, corrected *P*-values are shown. Raw data management was done in Microsoft Excel and statistical analyses were performed using GraphPad Prism 10.0 software.

Results

Mito-QC reporter provides sensitive detection of mitophagy and mitochondrial mass *in vitro* and *ex vivo*

The ARPE-19 cell line originated from the retinal pigment epithelium of a healthy adult donor, and underwent spontaneous immortalization ([Dunn et al., 1996](#)). ARPE-19 cells stably expressing the *mito*-QC reporter were used for all experiments ([Montava-Garriga et al., 2020](#)) and mitophagy levels were defined as the population of cells with an increased mCherry/GFP ratio ([Supplementary Figure S1](#)).



We treated *Park2*-expressing ARPE-19 cells with CCCP and DFP to validate the sensitivity of the reporter when analyzed by flow cytometry. CCCP is a protonophore that disrupts $\Delta\Psi_m$ by uncoupling the proton gradient, and is traditionally used as an inducer of PINK1/Parkin-mediated mitophagy (Narendra et al., 2008). DFP is an iron chelator that inhibits HIF-prolyl hydroxylases (PHDs), leading to HIF-1 α stabilization, hypoxia-like response and upregulation of downstream mitophagy regulators such as *BNIP3* or *BNIP3L/NIX* that engage in receptor-mediated mitophagy (Allen et al., 2013). Both compounds induced mitophagy at the 24 h timepoint, but only CCCP induced a significant increase after 6 h (Figures 1B, C).

Simultaneously, this reporter allows for quantification of mitochondrial mass defined by the mean fluorescence intensity (MFI) of its GFP component. CCCP significantly decreased cytosolic mitochondrial mass at both timepoints, but no changes were observed with DFP (Figures 1D, E). These results point to either a possible compensation by mitochondrial biogenesis to maintain homeostasis during receptor-mediated mitophagy or, since this pathway requires transcriptional activity to increase *BNIP3* and *BNIP3L/NIX* levels, that mitochondrial mass decrease will be observed at a later timepoint. In parallel, we performed a comparative analysis using spectral flow cytometry and obtained similar results regarding mitophagy levels (Supplementary Figure S2A) and mitochondrial mass (Supplementary Figure S2B) after mitophagy induction with CCCP and DFP, indicating that *mito-QC* can also be measured using this novel technology.

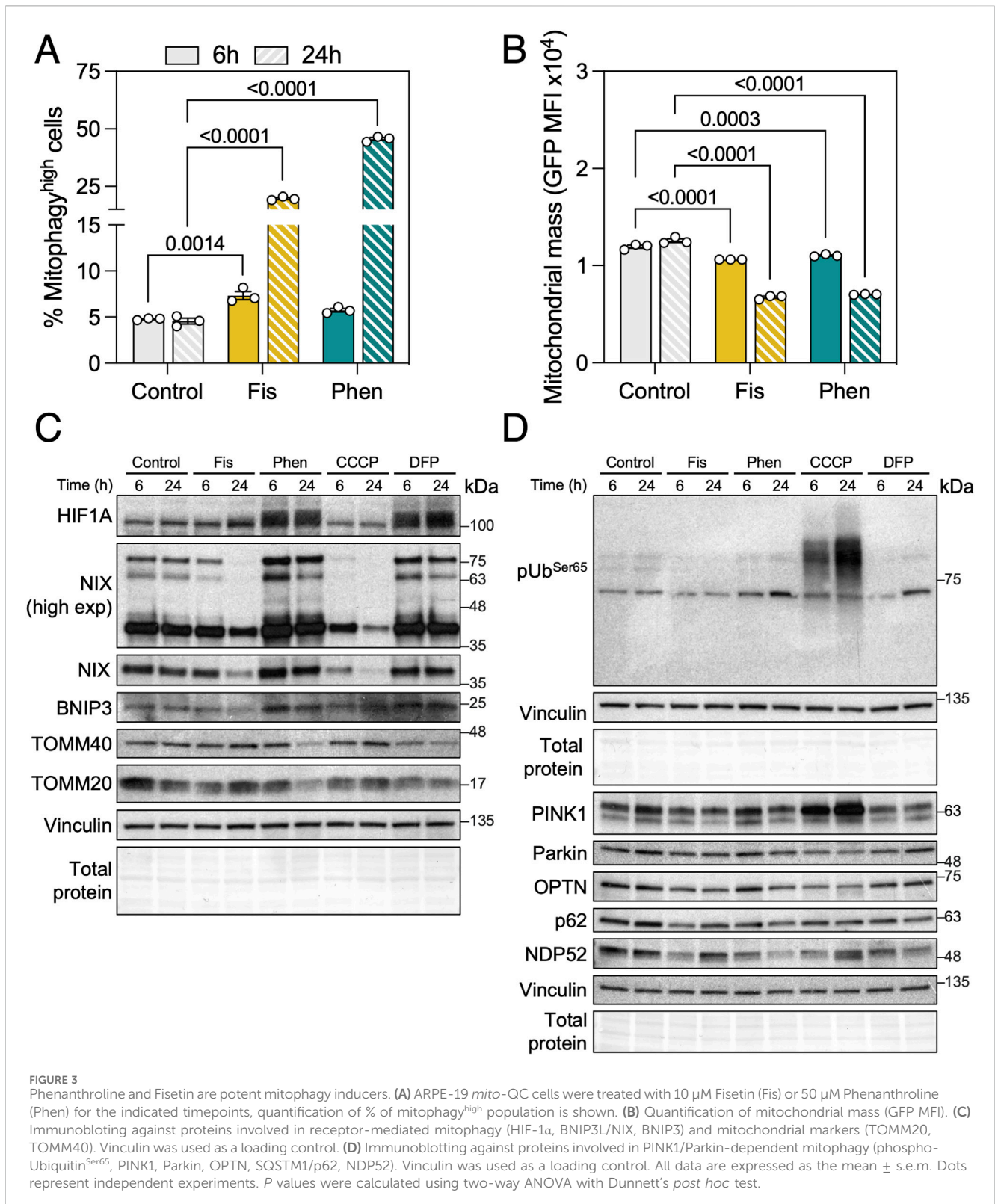
In addition, we also analyzed mitophagy in organotypic *ex vivo* retina culture from *mito-QC* mice (Figure 2A; Supplementary Figure S3). Replicating our findings *in vitro*, CCCP was able to induce mitophagy after 6 h of treatment but DFP was not (Figures 2B, C). The *mito-QC* reporter can therefore be used as a medium-throughput readout to assess mitophagy and mitochondrial mass *in vitro* and *ex vivo*.

Fisetin and phenanthroline induce mitophagy but no mitochondrial biogenesis

To further validate the use of the *mito-QC* reporter, we tested two compounds that we had previously found to significantly increase mitophagy using MitoTracker DeepRed flux assay: Fisetin and Phenanthroline (Mauro-Lizcano et al., 2015). Both compounds induced a robust mitophagy increase at 6 h that was exacerbated by 24 h (Figure 3A). With a similar kinetic to CCCP, both compounds significantly reduced mitochondrial mass at both timepoints analyzed suggesting no concomitant activation of mitochondrial biogenesis (Figure 3B). To further dissect the mechanism of action of these mitophagy inducers, we performed immunoblotting against the mediators of iron depletion-induced mitophagy and observed that Phenanthroline increased the protein levels of HIF-1 α and its downstream targets, the mitophagy receptors *BNIP3* and *BNIP3L/NIX* (Figure 3C). Fisetin decreased *BNIP3L/NIX* levels at the 24 h timepoint, but this observation might rather be representative of acute mitophagy as *BNIP3L/NIX* is a resident protein at the OMM (Wilhelm et al., 2022). We also evaluated PINK1 stabilization, phospho-Ubiquitin^{Ser65} and ubiquitin adaptor (OPTN, SQSTM1/p62, CALCOCO2/NDP52) levels but observed no differences with Fisetin nor Phenanthroline treatment (Figure 3D), indicating that their activity is PINK1/Parkin-independent.

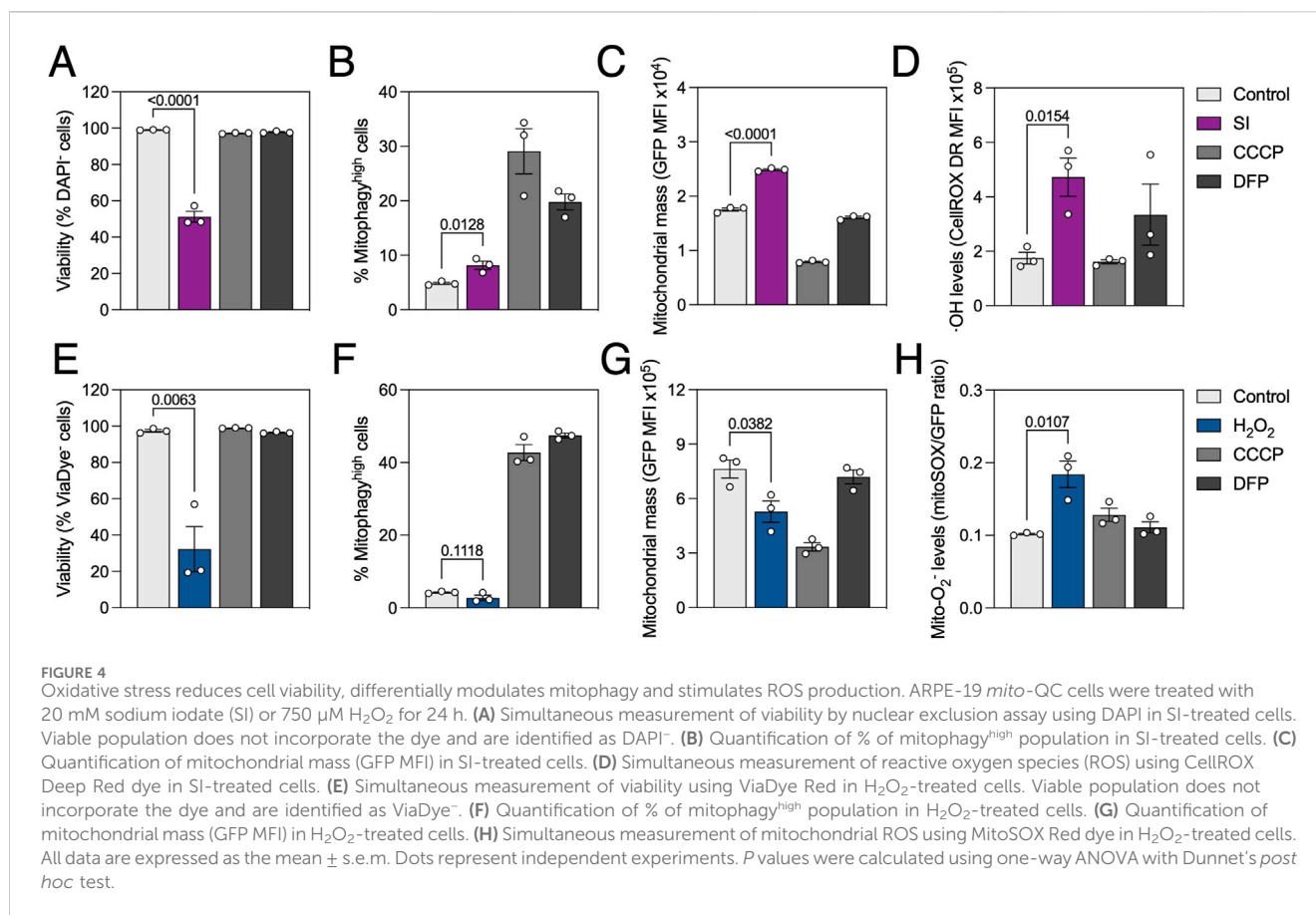
Mitophagy is impaired in an *in vitro* model of retinal degeneration

We previously described high mitophagy levels in the neuroretina and RPE (McWilliams et al., 2019; Jimenez-Loygorri et al., 2024). Sodium iodate (SI) is commonly used as a



pharmacological model of age-related macular degeneration (AMD), both *in vitro* and *in vivo* (Chowers et al., 2017). Even though AMD has been historically linked to mitochondrial dysfunction (Fisher and Ferrington, 2018) and impaired autophagy (Kaarniranta et al., 2023), evidence on the role of

mitophagy in AMD progression is scarcer (Jiménez-Loygorri et al., 2023). Using *mito*-QC analysis by flow cytometry we observed that treatment with SI for 24 h slightly increased mitophagy levels (Figure 4A) concomitant with a moderate but significant increase in mitochondrial mass (Figure 4B). Traditional



flow cytometers additionally equipped with violet and red lasers allow for multiplexing with additional dyes. We combined *mito*-QC readout with DAPI ($\lambda_{\text{ex}} = 350$ nm; $\lambda_{\text{em}} = 465$ nm), for nuclear exclusion viability assessment, and CellROX Deep Red ($\lambda_{\text{ex}} = 644$ nm; $\lambda_{\text{em}} = 665$ nm), a fluorogenic probe with high sensitivity for OH radical detection. SI decreased cell viability to ~70% (Figure 4C) and stimulated ROS production (Figure 4D), in line with previously published data (Chan et al., 2019).

Taking advantage of spectral flow cytometry which can detect the whole emission spectrum under different excitation lasers and dissect the contribution of every fluorophore, we also combined *mito*-QC with traditional red-emitting fluorescent probes. Treatment with H₂O₂ significantly decreased viability to ~40%, measured using ViaDye Red ($\lambda_{\text{ex}} = 615$ nm; $\lambda_{\text{em}} = 740$ nm) which binds to intracellular proteins when the plasma membrane is compromised (Figure 4E). While no changes were observed regarding mitophagy levels (Figure 4F), mitochondrial mass was decreased in H₂O₂-treated cells (Figure 4G). These observations were concurrent with increased mitochondrial O₂⁻ production, measured using MitoSOX Red dye ($\lambda_{\text{ex}} = 396$ nm; $\lambda_{\text{em}} = 610$ nm; Figure 4H). Markedly, all results were replicated in wild-type ARPE-19 cells using the same dyes (Supplementary Figures S4A, C) and MitoTracker Deep Red ($\lambda_{\text{ex}} = 644$ nm; $\lambda_{\text{em}} = 665$ nm) as a surrogate to measure mitochondrial mass (Supplementary Figure S4B). Spectral unmixing overcomes partial spectrum overlap and allows for simultaneous measurement of *mito*-QC and probes with similar fluorescence profiles.

Discussion

In the present manuscript we provide a standardized protocol to assess mitophagy in cells and *ex vivo* dissociated tissue using the tandem fluorescent *mito*-QC reporter via flow cytometry. Our results with *mito*-QC validate the ability of CCCP and Fisetin to stimulate mitophagy flux, as previously reported by our group using the MitoTracker Deep Red approach (Esteban-Martinez et al., 2017b), and now show that Phenanthroline also induces mitophagy in ARPE-19 cells. Finally, we highlight the possibility of simultaneously measuring other mitochondrial or intracellular parameters using additional probes and conventional or spectral flow cytometry. We also report that mitophagy is impaired in cell type-relevant oxidative stress models (SI, H₂O₂). Furthermore, the use of *mito*-QC bypasses the need for lysosomal degradation inhibitors (Mauro-Lizcano et al., 2015) and the putative confounding effects of drug or ROS interaction MitoTracker dye (Xiao et al., 2016).

The analysis of *mito*-QC by flow cytometry has been crucial for key findings such as the metabolic readaptation following iron chelation (Long et al., 2022) or to understand the interplay between BNIP3L/NIX-mediated mitophagy and pexophagy (Wilhelm et al., 2022). While protocols to measure mitophagy by flow cytometry using mt-Keima are readily available (Um et al., 2018; Winsor et al., 2020), this is, to our knowledge, the first protocol focused on the next-generation fixable *mito*-QC reporter. Compared to mt-Keima, the possibility of fixing *mito*-QC opens the possibility

of implementing, for example, flow cytometry immunophenotyping strategies to assess mitophagy in specific cell subsets within a heterogeneous sample. A novel tandem reporter called SRAI (Signal-Retaining Autophagy Indicator) composed of a pH-insensitive CFP variant (TOLLES) and a highly pH-sensitive YFP variant (YPet) has recently been developed and utilized to measure both mitophagy (Katayama et al., 2020) and ER-phagy (Jimenez-Moreno et al., 2023) *in vitro* or using viral vector delivery *in vivo*. There are also published guidelines on how to measure mitochondrial turnover using MitoTimer (Hernandez et al., 2013), but interpretation of data using MitoTimer should be cautious as it does not directly report mitochondria degradation within lysosomes (Gottlieb and Stotland, 2015).

While previous reports have raised concerns regarding the evaluation of PINK1/Parkin-dependent mitophagy using the *mito*-QC reporter (Liu et al., 2021), our results show that CCCP induced detectable levels of mitophagy as early as 6 h in ARPE-19 *mito*-QC cells. Similarly, we have previously reported an increase in mCherry⁺GFP⁻ mitolysosomes in response to Antimycin + Olygomycin (AO), another classical inducer of the PINK1/Parkin-dependent mitophagy pathway (Rosignol et al., 2020).

Phenanthroline is a metal ion chelator commonly used as a ligand in the chemical industry (Park et al., 2012). It had previously been suggested that phenanthroline induces severe DNMI1/DRP1-dependent mitochondrial fragmentation that leads to mitophagy (Park et al., 2012). We have now further characterized its mechanism of action showing that phenanthroline induces HIF-1 α stabilization and transcription of downstream mitophagy receptors BNIP3L/NIX and BNIP3. Interestingly, in our previous work we found that phenanthroline was not able to induce mitophagy in neuroblastoma-derived SH-SY5Y cells (Mauro-Lizcano et al., 2015) but a 10-fold increase was observed in ARPE-19 cells, indicating that its effect might be cell type-dependent. Phenanthroline has also been proposed as a pro-survival agent against apoptosis (Maitra et al., 2021) and parthanatos-mediated cell death (Chiu et al., 2012).

Fisetin is a natural flavonoid that acts as a potent SIRT1 NAD⁺-dependent histone deacetylase activator (Jang et al., 2012). The NAD⁺/NADH ratio is affected by mitochondrial function, and *vice versa* (Lautrup et al., 2024). Fisetin has been described to increase the NAD⁺/NADH ratio and induce mitophagy (Jang et al., 2012), through a mechanism that was dependent on the ubiquitin adaptor SQSTM1/p62 (Molagoda et al., 2021). Despite a robust increase in mitophagy in SH-SY5Y (Mauro-Lizcano et al., 2015) and ARPE-19 cells, we did not observe any changes in traditional PINK1/Parkin-dependent or receptor-mediated mitophagy effectors. The mechanism of action of Fisetin remains to be elucidated, but it has shown neuroprotective effects in models of neuroinflammation involving NLRP3 inflammasome activation (Molagoda et al., 2021; Ding et al., 2022). Both compounds showed no signs of cytotoxicity *in vitro* and warrant further exploration in diseases involving impaired mitophagy.

Previous evidence in the literature was suggestive of impaired autophagy in the SI model of AMD-associated geographic atrophy (Chan et al., 2019). In the present manuscript we indeed observed a slight increase in mitophagy but also a concomitant accumulation of mitochondria in the viable population of cells challenged with SI, replicating our previous findings using *mito*-

QC immunofluorescence (Jimenez-Loygorri et al., 2024). Primary RPE cultures from patients with AMD similarly display marked mitochondrial dysfunction (Ferrington et al., 2017) as well as autophagy defects (Ye et al., 2016) that could be a result of dysfunctional mitophagy. Boosting mitophagy could therefore be a novel potential therapeutic strategy in the prevention and/or treatment of AMD.

Finally, we also performed a comparison between widely available standard flow cytometry and spectral cytometry, exploring its added value. Polychromatic flow cytometry or standard flow cytometry is based on the principle one detector, one fluorochrome thanks to a series of dichroic filters. So, only a portion of the emitting signal can be collected. Spectral flow cytometry can collect the full fluorescence spectrum of every cell allowing the separation and differentiation among their spectral signatures, allowing more elaborate, multiplexed assays. This is possible thanks to the spectral unmixing algorithm which identifies the spectral signature of every fluorochrome plus the autofluorescence of the cells and resolves the complete spectra of every cell based on these parameters, allowing to differentiate the contribution of each fluorochrome in a certain wavelength (Robinson, 2022). Using this methodology, we were able to combine *mito*-QC analysis with green- and red-emitting intracellular probes that present partial spectral overlap with GFP and mCherry (Supplementary Figure S5).

Mitophagy analysis by flow cytometry, using *mito*-QC or similar reporters, therefore represents an update to previously used methodology, reducing time, cost and resources when compared to traditional microscopy analysis. Herein we provide a standardized protocol for *mito*-QC analysis using traditional and spectral flow cytometry, multiplexing with an array of intracellular probes and insight on mitophagy regulation using two inducers and models of oxidative stress.

Summary blurb

mito-QC reporter analysis by flow cytometry is a reliable and semi-high throughput method to measure mitophagy *in vitro* and *ex vivo*.

Data availability statement

The raw data supporting the conclusions of this article will be made available by the authors, without undue reservation.

Ethics statement

Ethical approval was not required for the studies on humans in accordance with the local legislation and institutional requirements because only commercially available established cell lines were used. The animal study was approved by Margarita Salas Center for Biological Research Bioethics Committee and Comunidad de Madrid (PROEX 154.3/21). The study was conducted in accordance with the local legislation and institutional requirements.

Author contributions

JJ-L: Conceptualization, Data curation, Formal Analysis, Investigation, Methodology, Validation, Visualization, Writing—original draft, Writing—review and editing. CJ-G: Formal Analysis, Investigation, Methodology, Visualization, Writing—original draft, Writing—review and editing. ÁV-P: Formal Analysis, Investigation, Writing—review and editing. PB: Conceptualization, Funding acquisition, Project administration, Resources, Supervision, Writing—review and editing.

Funding

The author(s) declare that financial support was received for the research, authorship, and/or publication of this article. Research in the PB lab is supported by grants 310030_215271 Swiss National Science Foundation (SNSF) and PID2021-126864NB I00 from MCIN, Spain. JJ-L holds a FPI fellowship from MCIN (PRE2019-088222). CJ-G is supported by the University of Fribourg.

Acknowledgments

We thank Ian Ganley for generating and providing the *mito*-QC reporter mice and *mito*-QC ARPE-19 cell lines; the animal facility (Angélica Horrillo, María Tijero) at the CIB Margarita Salas; the

References

- Allen, G. F., Toth, R., James, J., and Ganley, I. G. (2013). Loss of iron triggers PINK1/Parkin-independent mitophagy. *EMBO Rep.* 14 (12), 1127–1135. doi:10.1038/embor.2013.168
- Chan, C. M., Huang, D. Y., Sekar, P., Hsu, S. H., and Lin, W. W. (2019). Reactive oxygen species-dependent mitochondrial dynamics and autophagy confer protective effects in retinal pigment epithelial cells against sodium iodate-induced cell death. *J. Biomed. Sci.* 26 (1), 40. doi:10.1186/s12929-019-0531-z
- Chiu, S. C., Huang, S. Y., Tsai, Y. C., Chen, S. P., Pang, C. Y., Lien, C. F., et al. (2012). Poly (ADP-ribose) polymerase plays an important role in intermittent hypoxia-induced cell death in rat cerebellar granule cells. *J. Biomed. Sci.* 19 (1), 29. doi:10.1186/1423-0127-19-29
- Chowers, G., Cohen, M., Marks-Ohana, D., Stika, S., Eijzenberg, A., Banin, E., et al. (2017). Course of sodium iodate-induced retinal degeneration in albino and pigmented mice. *Invest. Ophthalmol. Vis. Sci.* 58 (4), 2239–2249. doi:10.1167/iovs.16-21255
- Ding, H., Li, Y., Chen, S., Wen, Y., Zhang, S., Luo, E., et al. (2022). Fisetin ameliorates cognitive impairment by activating mitophagy and suppressing neuroinflammation in rats with sepsis-associated encephalopathy. *CNS Neurosci. Ther.* 28 (2), 247–258. doi:10.1111/cns.13765
- Dunn, K. C., Aotaki-Keen, A. E., Putkey, F. R., and Hjelmeland, L. M. (1996). ARPE-19, a human retinal pigment epithelial cell line with differentiated properties. *Exp. Eye Res.* 62 (2), 155–169. doi:10.1006/exer.1996.0020
- Esteban-Martinez, L., Sierra-Filardi, E., McGreal, R. S., Salazar-Roa, M., Marino, G., Seco, E., et al. (2017a). Programmed mitophagy is essential for the glycolytic switch during cell differentiation. *EMBO J.* 36 (12), 1688–1706. doi:10.15252/embj.201695916
- Esteban-Martinez, L., Villarejo-Zori, B., and Boya, P. (2017b). Cytofluorometric assessment of mitophagic flux in mammalian cells and tissues. *Methods Enzymol.* 588, 209–217. doi:10.1016/bs.mie.2016.09.081
- Ferrington, D. A., Ebeling, M. C., Kapphahn, R. J., Terluk, M. R., Fisher, C. R., Polanco, J. R., et al. (2017). Altered bioenergetics and enhanced resistance to oxidative stress in human retinal pigment epithelial cells from donors with age-related macular degeneration. *Redox Biol.* 13, 255–265. doi:10.1016/j.redox.2017.05.015
- Figueiredo-Pereira, C., Villarejo-Zori, B., Cipriano, P. C., Tavares, D., Ramirez-Pardo, I., Boya, P., et al. (2023). Carbon monoxide stimulates both mitophagy and mitochondrial biogenesis to mediate protection against oxidative stress in astrocytes. *Mol. Neurobiol.* 60 (2), 851–863. doi:10.1007/s12035-022-03108-7
- Fisher, C. R., and Ferrington, D. A. (2018). Perspective on AMD pathobiology: a bioenergetic crisis in the RPE. *Invest. Ophthalmol. Vis. Sci.* 59 (4), AMD41–AMD47. doi:10.1167/iovs.18-24289
- Gomez-Sintes, R., Villarejo-Zori, B., Serrano-Puebla, A., Esteban-Martinez, L., Sierra-Filardi, E., Ramirez-Pardo, I., et al. (2017). Standard assays for the study of autophagy in the *ex vivo* retina. *Cells* 6 (4), 37. doi:10.3390/cells6040037
- Gottlieb, R. A., and Stotland, A. (2015). MitoTimer: a novel protein for monitoring mitochondrial turnover in the heart. *J. Mol. Med. Berl.* 93 (3), 271–278. doi:10.1007/s00109-014-1230-6
- Hasson, S. A., Kane, L. A., Yamano, K., Huang, C. H., Sliter, D. A., Buehler, E., et al. (2013). High-content genome-wide RNAi screens identify regulators of parkin upstream of mitophagy. *Nature* 504 (7479), 291–295. doi:10.1038/nature12748
- Hernandez, G., Thornton, C., Stotland, A., Lui, D., Sin, J., Ramil, J., et al. (2013). MitoTimer: a novel tool for monitoring mitochondrial turnover. *Autophagy* 9 (11), 1852–1861. doi:10.4161/auto.26501
- Jang, S. Y., Kang, H. T., and Hwang, E. S. (2012). Nicotinamide-induced mitophagy: event mediated by high NAD⁺/NADH ratio and SIRT1 protein activation. *J. Biol. Chem.* 287 (23), 19304–19314. doi:10.1074/jbc.M112.363747
- Jiménez-Loygorri, J. I., Benítez-Fernández, R., Viedma-Poyatos, Á., Zapata-Muñoz, J., Villarejo-Zori, B., Gómez-Sintes, R., et al. (2023). Mitophagy in the retina: viewing mitochondrial homeostasis through a new lens. *Prog. Retin Eye Res.* 96, 101205. doi:10.1016/j.preteyeres.2023.101205
- Jimenez-Loygorri, J. I., and Boya, P. (2024). Aging STINGs: mitophagy at the crossroads of neuroinflammation. *Autophagy* 20 (7), 1684–1686. doi:10.1080/15548627.2024.2322421
- Jimenez-Loygorri, J. I., Viedma-Poyatos, A., Gomez-Sintes, R., and Boya, P. (2024). Urolithin A promotes p62-dependent lysophagy to prevent acute retinal neurodegeneration. *Mol. Neurodegener.* 19 (1), 49. doi:10.1186/s13024-024-00739-3
- Jimenez-Moreno, N., Salomo-Coll, C., Murphy, L. C., and Wilkinson, S. (2023). Signal-retaining autophagy indicator as a quantitative imaging method for ER-phagy. *Cells* 12 (8), 1134. doi:10.3390/cells12081134
- Kaarniranta, K., Blasiak, J., Liton, P., Boulton, M., Klionsky, D. J., and Sinha, D. (2023). Autophagy in age-related macular degeneration. *Autophagy* 19 (2), 388–400. doi:10.1080/15548627.2022.2069437

flow cytometry facility at the CIB Margarita Salas and University of Fribourg (Patricia Yagüe and Sarah Cattin, respectively); Beatriz Villarejo-Zori for advice on *ex vivo* experiments and all members of the Autophagy Lab for thoughtful discussions and support.

Conflict of interest

The authors declare that the research was conducted in the absence of any commercial or financial relationships that could be construed as a potential conflict of interest.

Publisher's note

All claims expressed in this article are solely those of the authors and do not necessarily represent those of their affiliated organizations, or those of the publisher, the editors and the reviewers. Any product that may be evaluated in this article, or claim that may be made by its manufacturer, is not guaranteed or endorsed by the publisher.

Supplementary material

The Supplementary Material for this article can be found online at: <https://www.frontiersin.org/articles/10.3389/fcell.2024.1460061/full#supplementary-material>

- Katayama, H., Hama, H., Nagasawa, K., Kurokawa, H., Sugiyama, M., Ando, R., et al. (2020). Visualizing and modulating mitophagy for therapeutic studies of neurodegeneration. *Cell* 181 (5), 1176–1187. doi:10.1016/j.cell.2020.04.025
- Lautrup, S., Hou, Y., Fang, E. F., and Bohr, V. A. (2024). Roles of NAD(+) in health and aging. *Cold Spring Harb. Perspect. Med.* 14 (1), a041193. doi:10.1101/cshperspect.a041193
- Lazarou, M., Sliter, D. A., Kane, L. A., Sarraf, S. A., Wang, C., Burman, J. L., et al. (2015). The ubiquitin kinase PINK1 recruits autophagy receptors to induce mitophagy. *Nature* 524 (7565), 309–314. doi:10.1038/nature14893
- Liu, Y. T., Sliter, D. A., Shammas, M. K., Huang, X., Wang, C., Calvelli, H., et al. (2021). Mt-Keima detects PINK1-PRKN mitophagy *in vivo* with greater sensitivity than mito-QC. *Autophagy* 17 (11), 3753–3762. doi:10.1080/15548627.2021.1896924
- Long, M., Sanchez-Martinez, A., Longo, M., Suomi, F., Stenlund, H., Johansson, A. I., et al. (2022). DGAT1 activity synchronises with mitophagy to protect cells from metabolic rewiring by iron depletion. *EMBO J.* 41 (10), e109390. doi:10.15252/embj.2021109390
- Maitra, S., Sornjai, W., Smith, D. R., and Vincent, B. (2021). Phenanthroline impairs β APP processing and expression, increases p53 protein levels and induces cell cycle arrest in human neuroblastoma cells. *Brain Res. Bull.* 170, 29–38. doi:10.1016/j.brainresbull.2021.02.001
- Mauro-Lizcano, M., Esteban-Martinez, L., Seco, E., Serrano-Puebla, A., Garcia-Ledo, L., Figueiredo-Pereira, C., et al. (2015). New method to assess mitophagy flux by flow cytometry. *Autophagy* 11 (5), 833–843. doi:10.1080/15548627.2015.1034403
- McWilliams, T. G., Prescott, A. R., Montava-Garriga, L., Ball, G., Singh, F., Barini, E., et al. (2018). Basal mitophagy occurs independently of PINK1 in mouse tissues of high metabolic demand. *Cell Metab.* 27 (2), 439–449. doi:10.1016/j.cmet.2017.12.008
- McWilliams, T. G., Prescott, A. R., Villarejo-Zori, B., Ball, G., Boya, P., and Ganley, I. G. (2019). A comparative map of macroautophagy and mitophagy in the vertebrate eye. *Autophagy* 15 (7), 1296–1308. doi:10.1080/15548627.2019.1580509
- Molagoda, I. M. N., Athapaththu, A., Choi, Y. H., Park, C., Jin, C. Y., Kang, C. H., et al. (2021). Fisetin inhibits NLRP3 inflammasome by suppressing TLR4/MD2-mediated mitochondrial ROS production. *Antioxidants (Basel)* 10 (8), 1215. doi:10.3390/antiox10081215
- Montava-Garriga, L., Singh, F., Ball, G., and Ganley, I. G. (2020). Semi-automated quantitation of mitophagy in cells and tissues. *Mech. Ageing Dev.* 185, 111196. doi:10.1016/j.mad.2019.111196
- Narendra, D., Tanaka, A., Suen, D. F., and Youle, R. J. (2008). Parkin is recruited selectively to impaired mitochondria and promotes their autophagy. *J. Cell Biol.* 183 (5), 795–803. doi:10.1083/jcb.200809125
- Narendra, D. P., Jin, S. M., Tanaka, A., Suen, D. F., Gautier, C. A., Shen, J., et al. (2010). PINK1 is selectively stabilized on impaired mitochondria to activate Parkin. *PLoS Biol.* 8 (1), e1000298. doi:10.1371/journal.pbio.1000298
- Nguyen, T. N., Padman, B. S., and Lazarou, M. (2016). Deciphering the molecular signals of PINK1/parkin mitophagy. *Trends Cell Biol.* 26 (10), 733–744. doi:10.1016/j.tcb.2016.05.008
- Park, S. J., Shin, J. H., Kim, E. S., Jo, Y. K., Kim, J. H., Hwang, J. J., et al. (2012). Mitochondrial fragmentation caused by phenanthroline promotes mitophagy. *FEBS Lett.* 586 (24), 4303–4310. doi:10.1016/j.febslet.2012.10.035
- Robinson, J. P. (2022). Flow cytometry: past and future. *Biotechniques* 72 (4), 159–169. doi:10.2144/btn-2022-0005
- Rosignol, I., Villarejo-Zori, B., Teresak, P., Sierra-Filardi, E., Pereiro, X., Rodriguez-Muela, N., et al. (2020). The mito-QC reporter for quantitative mitophagy assessment in primary retinal ganglion cells and experimental glaucoma models. *Int. J. Mol. Sci.* 21 (5), 1882. doi:10.3390/ijms21051882
- Teresak, P., Lapao, A., Subic, N., Boya, P., Elazar, Z., and Simonsen, A. (2022). Regulation of PRKN-independent mitophagy. *Autophagy* 18 (1), 24–39. doi:10.1080/15548627.2021.1888244
- Um, J. H., Kim, Y. Y., Finkel, T., and Yun, J. (2018). Sensitive measurement of mitophagy by flow cytometry using the pH-dependent fluorescent reporter mt-keima. *J. Vis. Exp.* 138, 58099. doi:10.3791/58099
- Wilhelm, L. P., Zapata-Muñoz, J., Villarejo-Zori, B., Pellegrin, S., Freire, C. M., Toye, A. M., et al. (2022). BNIP3L/NIX regulates both mitophagy and pexophagy. *Embo J.* 41 (24), e111115. doi:10.15252/embj.2022111115
- Winsor, N. J., Killackey, S. A., Philpott, D. J., and Girardin, S. E. (2020). An optimized procedure for quantitative analysis of mitophagy with the mtKeima system using flow cytometry. *Biotechniques* 69 (4), 249–256. doi:10.2144/btn-2020-0071
- Xiao, B., Deng, X., Zhou, W., and Tan, E. K. (2016). Flow cytometry-based assessment of mitophagy using MitoTracker. *Front. Cell Neurosci.* 10, 76. doi:10.3389/fncel.2016.00076
- Ye, F., Kaneko, H., Hayashi, Y., Takayama, K., Hwang, S. J., Nishizawa, Y., et al. (2016). Malondialdehyde induces autophagy dysfunction and VEGF secretion in the retinal pigment epithelium in age-related macular degeneration. *Free Radic. Biol. Med.* 94, 121–134. doi:10.1016/j.freeradbiomed.2016.02.027